Glycine self-assembled on graphene enhances the solar absorbance performance

Fatih Ersan [a, b], Ethem Aktürk [a, c, *], Salim Ciraci [b, **]

[a] Department of Physics, Adnan Menderes University, 09100, Aydın, Turkey
[b] Department of Physics, Bilkent University, Ankara, 06800, Turkey
[c] Nanotechnology Application and Research Center, Adnan Menderes University, Aydın, 09010, Turkey

ABSTRACT

Despite its high solar absorbance and surface coating abilities, pristine graphene as a semimetal is not promising for photovoltaic applications. In this study, we predict that Glycine (Gly), an amino acid, which is normally bound to pristine graphene by a weak van der Waals attraction, can form an organic coating durable to ambient condition when adsorbed on vacancy patterned graphene surface. Moreover, adsorbed Gly coating induces metal-insulator transition and concomitantly increases the solar absorbance of pristine graphene more than three times. This way, graphene attain critical functionalities to be used in solar energy and photovoltaic applications.

© 2018 Elsevier Ltd. All rights reserved.

1. Introduction

Unusual mechanical, electronic and optoelectronic properties of ultrathin, two-dimensional (2D) materials have developed diverse fields of research for new technological applications. One critical field has been the conversion of the energy of the sun light to the electrical energy on solar panels through photovoltaic effects. Earlier research has demonstrated that 2D materials like graphene, h-MoS_2 enhance the solar absorbance significantly, that have been exploited actively to increase the efficiency of the solar panels. For example, a monolayer of graphene of 3.2 Å thickness can absorb 2.3% of incident white light [1,2]. This value is nearly equivalent to the absorbance of a 20 nm thick Si or 5–10 nm thick GaAs films [3]. Monolayers of transition metal dichalcogenides (TMDC), such as MoS_2, $MoSe_2$, WS_2 and their alloys can absorb up to 5–10% incident sunlight even if their thicknesses are less than 1 nm [3,4].

While semimetallic graphene has been exploited in the area closely related with energy, such as high capacity hydrogen storage [5,6] and nanoscale dielectric capacitors [7,8], it may not be an attractive material in energy conversion despite its high solar absorbance. Nonetheless, efforts have continued to utilize graphene in efficient organic photovoltaic (OPV) and dye sensitized solar cells as an electrode or an active layer [9,10]. For example, Choe et al. [11] reported that the performance of OPVs with multilayer graphene films was found to be the best with power conversion efficiency of 1.3%. Park et al. [12] reported that the overall power conversion efficiency of organic solar cells can be enhanced by $AuCl_3$ doping on graphene films. In addition, Valentini et al. [13] showed that the butylamine modified graphene sheets can enhance the charge carrier transport in polymer photovoltaic applications. In spite of recent advances in the applications of graphene or graphene-based materials in organic photovoltaic cells, the molecular mechanism of the chemically modified graphene based OPVs are still unclear. In this respect, the development of novel functionalized graphene to be used as electrodes in solar cells, is of great importance. On the other side, Shih et al. [14] showed that photovoltaic performance of perovskite solar cells, which are modified by amino acids can be enhanced. In fact, perovskite solar cell devices modified by glycine (Gly) have exhibited a superior power conversion efficiency relative to bare devices. In this respect, the power conversion efficiency of Gly modified $TiO_2/CH_3NH_3PbI_3$ heterojunction was shown [15] to increase from 8.35 to 12.02 %.

In this paper, the coating of an organic molecule, Gly is investigated to make graphene functional in solar energy conversion. Gly, NH_2CH_2COOH, is an amino acid being one of the principal

* Corresponding author. Department of Physics, Adnan Menderes University, 09100, Aydın, Turkey.
** Corresponding author.
E-mail addresses: ethem.akturk@adu.edu.tr (E. Aktürk), ciraci@fen.bilkent.edu.tr (S. Ciraci).

ingredients of protein. On pristine graphene surface, Gly is normally bound only by a weak van der Waals attraction of 0.5–0.4 eV and is prone to diffuse or dissociate. However, as shown in our recent study, when it is bound to one or two-fold coordinated C atoms at the edge of a defect, like a monovacancy, reconstructions can be induced and eventually strong chemical bonds can form between Gly and graphene.[16] A mesh of defects in graphene, such as periodic holes (graphene nanomeshes) [17], carbon monovacancies [18], or Stone-Wales in graphene [19] can be created by ion irradiation techniques, whereby the semimetallic graphene is transformed into a magnetic metal and its durable coating with Gly is enabled. Here, we found that defect patterned graphene changes into a semiconductor and concomitantly its solar absorbance is further increased, when covered by Gly. This important and novel result obtained by performing state-of the-art density functional theory (DFT) calculations shows how graphene can be utilized in efficient solar energy conversion through an organic coating.

2. Computational details

First-principles spin-polarized plane wave calculation were carried out within density functional theory using projector augmented-wave (PAW) potentials [20]. Exchange-correlation potential approximated by generalized gradient approximation (GGA) using Perdew, Burke and Ernzerhof (PBE) functional [21] including van der Waals (vdW) corrections in D2 level (D2-G) [22]. Wave functions are expanded in plane-wave basis sets up to electron kinetic energy cut-off of 650 eV. Single Gly bound to the pristine graphene or to a defect site like single vacancy are modeled by a (8×8) periodic supercell in xy-plane which are stacked along z-direction with a 15 Å vacuum spacing in order to avoid interlayer interactions. Brillouin zone (BZ) integration is performed with $(9 \times 9 \times 1)$ k-point mesh, following the convention of Monkhorst and Pack [23]. To investigate the ordered periodic monovacancies in graphene, rectangular supercells are created with the same vacuum spacing and $(6 \times 4 \times 1)$ k-point meshes used for these supercells. Ionic relaxation is realized by conjugated gradient algorithm [24], which optimizes structure without breaking symmetry. All atoms in the supercell are fully relaxed until the energy difference between the successive steps is less than 10^{-5} eV and the net force on each atom is less than 10^{-2} eV/Å. In addition, maximum pressure on the lattice has been lowered down to 1 kbar. Numerical calculations are carried out by using VASP software [25,26].

Thermal stability and desorption of specific structures are tested by ab-initio, finite temperature molecular dynamics (AIMD) calculations. A Nosé thermostat was used, and Newtonian equations of motion were integrated through the Verlet algorithm with time steps of 2 fs for 1000 iterations. The energy barrier between the initial and final configurations are determined by using climbing image nudged elastic band (CI-NEB) method [27].

Local field and excitonic effects are not included in our calculations, where Γ-centered, $(8 \times 6 \times 1)$ k-points mesh and 140 empty bands in addition to the valence bands of each graphene + glycine structures. To compare the absorbance spectrums of the optimized graphene + glycine structures with the incident sunlight, we used AM1.5 G reference solar spectral irradiance [28].

3. Results

3.1. Glycine and its interaction with graphene

Glycine (Gly) is the simplest amino acid which plays an important role for building other long-chain, complex amino acid structures. Gly can exits either in a neutral [29] form in the gas phase (see Fig. 1a) or in a zwitterionic [30] form in aqueous solution.

Calculated bond lengths and energy levels are illustrated in Fig. 1a, which are in fair agreements with experimental data [29]. As shown Gly has a wide HOMO-LUMO gap of $E_{g-HL} = 4.59$ eV calculated by PBE, which increases to 6.20 eV after Heyd-Scuseria-Ernzerhof (HSE) [31] correction. While *2p* orbitals of N atom dominate the HOMO state, LUMO state originates mainly from *2p*-orbitals of C atom. Other features of Gly, such as its vibration spectrum, interactions with pristine graphene and libration frequencies, zwitterionic states and metal-semiconductor heterostructure formation can be obtained from Ref.[16].

Pristine graphene is known to be inert to amino acids [32–34] as it does to many gas molecules like O_2, H_2 and CO [35]. For example, the binding energy of Gly adsorbed to the pristine graphene in lateral configuration is weak and is only ~0.5 eV. The majority of this energy emerges from attractive vdW interaction; only a small part of 80 meV originates from weak chemical bonding. These results are in agreement with the earlier calculations [16,36,37]. Whereas the binding of zwitterionic form of the Gly to graphene slightly stronger then its neutral form due to the polarization in the charge density distribution.

The reactivity of graphene can be enhanced by specific defects, like monovacancy or divacancy in graphene, due two fold coordinated C atoms with unsaturated sp^2-dangling bonds at the defect sites [16]. Accordingly, atoms or molecules, which are normally weakly bound to pristine graphene, can be adsorbed strongly on the defect site [35,38]. Two types of carbon monovacancy are distinguished in graphene; namely symmetric (S-1V) and reconstructed (R-1V) monovacancy. Although, R-1V seems to be energetically favorable, both types of monovacancies have been observed experimentally [39]. In the symmetric one, three two-folded C atoms surrounding the vacancy form an equilateral triangle, whereas in R-1V, two two-fold coordinated C atoms form a C-C bond leaving only one two-fold coordinated C atom with one dangling bond.

We first examine the adsorption of Gly to an isolated monovacancy and demonstrate that a strong bond formed between Gly and graphene pins the molecule on the surface. The isolated monovacancy is mimicked by a periodically repeating monovacancy in each $(8 \times 8 \times 1)$ supercell of graphene. Within this supercell geometry, the semimetallic pristine graphene turns to a metal and attains a magnetic moment by the creation of a monovacancy, for both S-1V and R-1V. The electronic energy band structure of R-1V shown in Fig. 1 b indicates the metallicity of the system, since the Fermi level dips below the top of the valence band. Upon the adsorption of Gly to isolated monovacancy, a chemical bond is formed between C-dangling bond and Gly, which strongly attaches the molecule to graphene. This way the sp^2-dangling bond of the two-fold coordinated C-atom at the vacancy site is saturated. This is followed by the opening a band gap, which transforms the system from metal to insulator (Fig. 1 c). The formation of this chemical bonding is corroborated by a Bader charge analysis showing significant charge transfer from Gly to graphene. Other binding configurations, such as the binding of Gly through CH or OH sites, the binding energies are relatively low (~0.8 eV), and not energetically favorable.

3.2. Self assembling of Gly on graphene

Strong binding of Gly on the R-1V graphene is critical for the self-assembly of an organic molecule and paves the way to the functionalization of graphene by organic molecules. Motivated with the controlled defect creation in the graphene by ion irradiation technique [17–19], we first consider one-dimesnional (1D) row and 2D mesh of patterned vacancy defects with well-defined repeat periods. Secondly, the adsorption of Glys on these
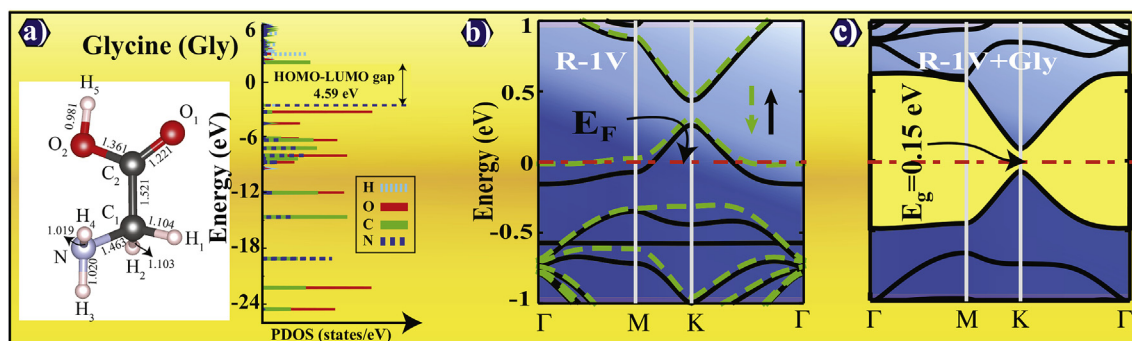
Fig. 1. (a) Atomic configuration of Glycine (Gly) with calculated bond lengths and its electronic energy spectrum with HOMO-LUMO band gap calculated within PBE. (b) Calculated electronic energy band structure of an isolated reconstructed monovacancy, R-1V, mimicked by a periodically repeating R-1V in each $(8 \times 8 \times 1)$ supercell of graphene. Fermi level below the top of the valence band indicates the metallicity of the system. (c) Upon adsorption, the sp^2-dangling bond of two-fold coordinated C atom at the defect site is saturated by Gly. This transforms the metallic system to a semiconductor by opening the band gap. Zero of energy is set at the Fermi level shown by dash-dotted line. (A colour version of this figure can be viewed online.)

patterned vacancies are examined to reveal whether they are self-assembled. In Fig. 2a and b, the adsorption of Gly to monovacancies forming a 1D and 2D patterned defects, respectively are shown. The first pattern has two and eight hexagons along x- and y-direction, respectively, whereby nearest vacancies along x-direction are kept adjacent to each other, while those along y-direction are wide separated. Therefore, this structure is considered to be one-dimensional and is specified as (2×8). The second pattern specified as (4×8) and considered to be 2D has four and eight hexagons along x- and y-direction, respectively, and has four Glys adsorbed. Similar patterns in 1D and 2D and specified as (3×8) and (6×8),

respectively are examined in Fig. 2c and d, where two nearest vacancies along x-direction are separated by one hexagon. It should be noted that in the vacancy patterns including single molecule in the cell, Glys are forced to have same orientation as in Fig. 2 a and c. To lift this constraint imposed by the periodic boundary conditions, the unit cells containing four Glys are used in Fig. 2 b and d. Following the optimizations of these four periodic structures Glys preferred to bind through their N atoms with a significant binding energy. One H atom dissociated from Gly saturated one of the dangling bonds, while Gly by itself saturated another dangling bond of C atom surrounding the vacancy. This way the
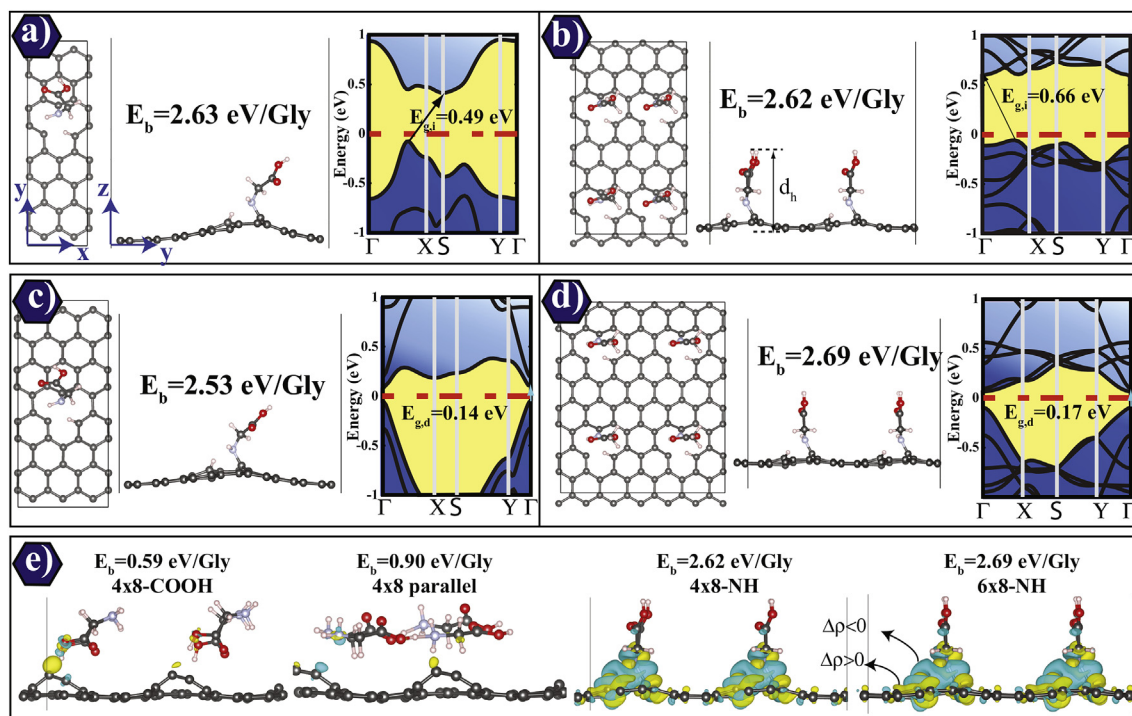

Fig. 2. Gly adsorbed (self-assembled) at the patterned vacancy defects repeated in various supercells.(a) (2×8)-NH supercell consisting of two and eight hexagons along x- and y-directions, one monovacancy and a Gly adsorbed through its N end. Upon adsorption, one H atom dissociated from Gly saturates one of C atoms around the vacancy and opens a band gap. Atomic configuration with binding energy E_b and resulting energy band structure are shown by insets. This structure is considered to be 1D, since the interaction along y-direction is negligible. (b) (4×8)-NH supercell exhibits a 2D behavior, since the interactions along x- and y-directions are comparable. (c) (3×8)-NH structure with one hexagon between two adjacent vacancies. (d) (6×8)-NH supercell constituting a 2D self-assembly of Gly at monovacancies having one hexagon between them along x-axis. (e) Isosurfaces of difference charge density of Gly adsorbed to (4×8)-COOH, (4×8)-parallel, (4×8)-NH and (6×8)-NH structures. Yellow zones indicates charge accumulation and blue for charge depletion. Isosurface level is set to 0.003 e/Å³. (A colour version of this figure can be viewed online.)

reconstruction of the symmetric vacancy is suppressed. If glycines come to approach the defected graphene from its COOH site, they just bind weakly to the surface as can be seen in Fig. 2 e. The bonding is analyzed in terms of the difference charge densities. Fig. 2 e illustrates the isosurfaces of difference charge density (obtained by subtracting free-atom charge densities from the self-consistent field, total charge density) of Gly adsorbed to (4×8) and (6×8) structures. To illustrate the difference charge densities we used VESTA [40] program. Strong charge rearrangements and local polarizations thereof indicate chemical binding, while weak interactions of Glys such as (4×8)-COOH and (4×8)-parallel structures give rise to minute charge rearrangements.

For the above four periodic structures binding configurations are similar and the binding energies range between 2.50 eV and 2.60 eV. Additionally, upon coverage of Gly, all structures underwent a metal-insulator transition attaining fundamental band gaps in the range of 0.14 eV−0.66 eV depending on the periodicity of the structures. While (2×8) and (4×8) structures with adjacent monovacancies, attained relatively large indirect band gaps, (3×8) and (6×8) structures with separated monovacancies have small direct fundamental band gaps. These bands calculated with PBE are expected to increase with HSE or GW self-energy corrections.

To test the self-assembly character, we deliberately changed/disturbed the adsorption geometry of one Gly among four Glys in the unit cell. Upon the reoptimization of the structure, all Glys kept their original configuration. This clearly demonstrates that Glys are adsorbed at the defect sites forming a specific pattern produce a strongly bound coating. It is noted that some configurations resulting with weak binding are not favored energetically. The strong binding of Glys on defect patterned graphene exhibiting a self-assembly character and dramatically modifying the substrate electronic properties is an important result and can lead to novel fields of application for graphene as explained in the forthcoming section.

3.2.1. Enhanced solar absorbance

As certified by experimental measurements, graphene is an excellent white light absorber with 2.3% absorbance ratio, despite its thickness of 3.2 Å [1,2]. Therefore, it is a 2D material suitable for various solar absorbance applications, whereas it cannot be used for photovoltaics due to its semimetallic band structure. Here we show that through the self-assembly of Gly on the defect patterned graphene one can achieve a coating of organic material sustaining ambient condition, which can change semimetallic graphene to a semiconductor and concomitantly further enhances its solar absorbance to make it attractive for photovoltaic applications.

First, we present our results related with the optical properties of Gly coated graphene. Fig. 3a illustrates the imaginary parts of the dielectric functions (ε_2) versus energy calculated for various coatings of Gly on the defect patterned graphene. The self-assembly patterns of these coatings are identified by different lines in the spectrum. For the sake of comparison, ε_2 versus energy of MoS$_2$ monolayer, which has extremely high absorbance value in the visible region of the electromagnetic spectrum [3,4], is also presented in the same figure. Note that the functions of ε_2 versus energy calculated for monolayers of graphene and MoS$_2$ are in agreement with the spectrums reported earlier [3,41]. As one clearly sees, values of ε_2 calculated for pristine graphene are enhanced upon coating of self-assembled Gly. The metal-insulator transition induced by the adsorbed Gly attributing a semiconducting behavior to the graphene + self-assembled Gly system is the cause of these enhancement. Electric displacement vector **D** is related to the polarization density **P** by the following expression, $\mathbf{D} = \varepsilon_0\mathbf{E} + \mathbf{P} = \varepsilon_0(1 + \chi_e)\mathbf{E} = \varepsilon_0\varepsilon_r\mathbf{E}$, where ε_0 is the dielectric constant of free space, **E** is the electric field, χ_e is the susceptibility
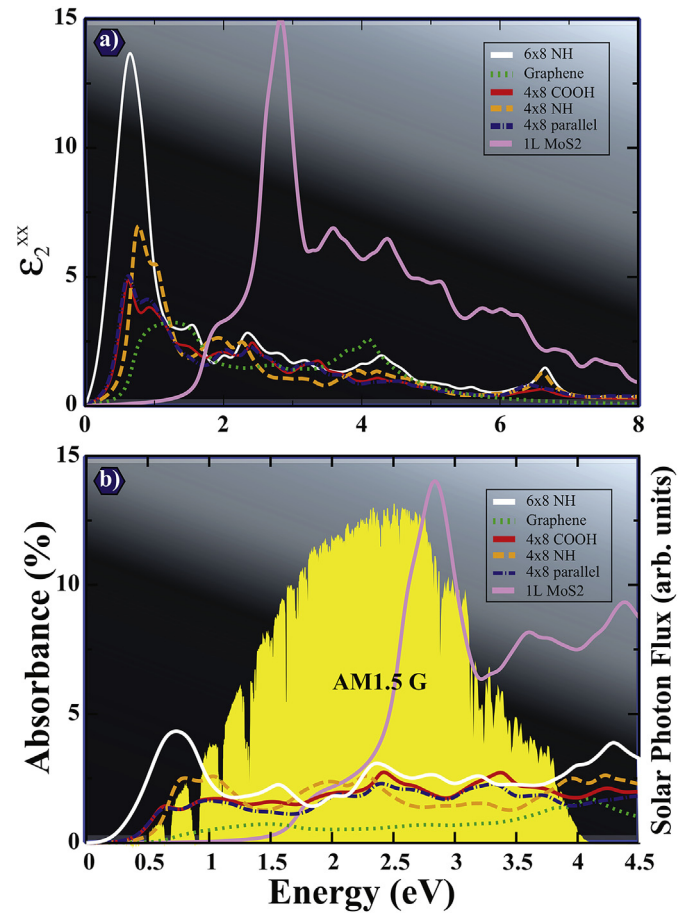

Fig. 3. (a) Imaginary part of dielectric constant, ε_2, versus energy calculated for Gly adsorbed on diverse vacancy patterned graphene surfaces. ε_2 calculated for pristine graphene and MoS$_2$ are presented for the sake of comparison. "xx" denotes the in-plane x-components of the dielectric function. (b) Same for the calculated solar absorbance curves versus energy. The curve of solar photon flux is shaded. (A colour version of this figure can be viewed online.)

of a medium and ε_r is the dielectric constant of the material. By changing the electronic structure from metal the semiconductor, bound charge in the structure increases as depicted in Fig. 2 e, which causes to high polarization in the system. The displacement vector of the structure gets larger, and hence ε_2 increases. Larger dielectric function causes to higher absorbance value. Absorbance of the ultra thin materials can be calculated from the expression, [3,4];

$$A(\omega) = \frac{\omega}{c}\varepsilon_2(\omega)\Delta z \qquad (1)$$

where, c is the speed of light, and Δz is the height of the simulation cell normal to the surface (or the thickness of the coating). This equation is obtained from the expression $A(\omega) = 1 - e^{-\alpha\Delta z}$ by using Taylor expansion in view of the fact that Δz is very small. In this study we assumed that Δz is the polarizable electronic thickness, which is obtained in terms of d_h (i.e. the total height of the graphene + Gly system as illustrated in Fig. 2b) and the van der Waals atomic radii of C and H atoms of the adsorbed Gly in the following equation [42];

$$\Delta z = d_h(graphene + Gly) + r_C^{vdW} + r_H^{vdW}. \qquad (2)$$

Fig. 3b illustrates the absorbance curves calculated for diverse self-assembly structures. Even if the absorbance values calculated

within PBE for the pristine graphene are underestimated relative to the experimental, its overall features and the positions of the peaks are in agreement with the experiments [2]. In fact, earlier studies on the optical properties of graphite and graphene [2,43,44] have demonstrated that advanced approaches with many-body self-energy correction and including the solution of the Bethe-Salpater equation (GW-BSE), can predict the position of the optical absorption peak of graphene in good agreement with the experimental peak, but overestimates the measured intensities by more than 30%. On the other hand, GW calculations overestimated the energy of the experimental peak position by 0.6 eV and its intensity by more than 30%. Therefore, given the convergence problems of advanced approaches, our calculations predicting the optical adsorption peak energy with down shifts of only 10%, and also representing experimental trends correctly provide rather good understanding of the physical phenomena.

Furthermore, our result for the absorbance of MoS_2 monolayer is in agreement with the previously reported curves [3,4]. As seen, self-assembly of Gly on the defect patterned graphene enhances also the absorbance more than three times. In particular, in the energy range from 0.5 eV to 1.6 eV, self-assembled structures show high absorbance, while MoS_2 monolayer has almost no absorbance due to its large band gap. Hence, these Gly coated graphene is expected to be suitable for the lower energy spectrum of the sunlight. Notably, 6×8-NH structure has the highest absorbance value up to 1 eV in the spectrum, while the absorbances of other structures in this range are suppressed due to their indirect fundamental band gaps. However, for energies higher than 1 eV, all of the structures have nearly same absorbance values. Similar situation occurs also for the monolayer MoS_2 having direct fundamental band gap; the photoluminescence (PL) of it is higher than MoS_2 thin film with indirect fundamental band gap [45,46]. As another example, germanium crystal is an indirect band-gap semiconductor, but its band gap turns to direct under biaxial tensile strain with an increase of its PL intensity [47].

4. Conclusion

Graphene well-known as a good coating material is also an efficient solar absorber; much better than silicon films. However, it does not promise much in photovoltaic application due to its semimetallic state. This disadvantageous situation can be remedied through the coating of the graphene surface by an organic molecule, Gly, which is an amino acid. Normally, pristine graphene weakly interact with Gly molecules through the van der Waals attraction, that makes the coating very weak and prone to dissociate in ambient conditions. We showed that Gly molecules can be pinned at the vacancy sites of graphene by forming strong chemical bonds. When adsorbed on patterned monovacancy, Gly changes the metallic Gly + graphene system to a semiconductor by forming an organic coating, which is durable to ambient conditions. In addition, the solar absorbance of the Gly coated graphene increases also more than three times relative to the pristine graphene. At the end, Gly coated graphene together with its other extraordinary properties becomes a critical 2D material in photovoltaics. We believe that our finding is important for the usage of graphene in solar energy applications.

Acknowledgments

References

[1] R.R. Nair, P. Blake, A.N. Grigorenko, K.S. Novoselov, T.J. Booth, T. Stauber, N.M.R. Peres, A.K. Geim, Fine structure constant defines visual transparency of graphene, Science 320 (5881) (2008) 1308.

[2] L. Yang, J. Deslippe, C.H. Park, M.L. Cohen, S.G. Louie, Excitonic effects on the optical response of graphene and bilayer graphene, Phys. Rev. Lett. 103 (2009) 186802.

[3] M. Bernardi, M. Palummo, J.C. Grossman, Extraordinary sunlight absorption and one nanometer thick photovoltaics using two-dimensional monolayer materials, Nano Lett. 13 (2013) 3664–3670.

[4] T.L. Tan, M.F. Ng, G. Eda, Stable monolayer transition metal dichalcogenide ordered alloys with tunable electronic properties, J. Phys. Chem. C 120 (2016) 2501–2508.

[5] E. Durgun, S. Ciraci, T. Yildirim, Functionalization of carbon-based nanostructures with light transition metal atoms for hydrogen storage, Phys. Rev. B 77 (2008), 085405.

[6] C. Ataca, E. Akturk, S. Ciraci, H. Ustunel, High-capacity hydrogen storage by metallized graphene, Appl. Phys. Lett. 93 (2008), 043123.

[7] V.O. Ozcelik, S. Ciraci, Nanoscale dielectric capacitors composed of graphene and boron nitride, J. Phys. Chem. C 117 (2013) 15327–15334.

[8] V.O. Ozcelik, S. Ciraci, High-performance planar nanoscale dielectric capacitors, Phys. Rev. B 91 (2015) 195445.

[9] X. Wan, G. Long, L. Huang, Y. Chen, Graphene-a promising material for organic photovoltaic cells, Adv. Mater. 23 (2011) 5342.

[10] D.W. Chang, H.-J. Choi, A. Filer, J.-B. Baek, Graphene in photovoltaic applications: organic photovoltaic cells (OPVs) and dye-sensitized solar cells (DSSCs), J. Mater. Chem. A 2 (2014) 12136.

[11] M. Choe, B.H. Lee, G. Jo, J. Park, W. Park, S. Lee, W.K. Hong, M.J. Seong, Y.H. Kahng, K. Lee, T. Lee, Efficient bulk-heterojunction photovoltaic cells with transparent multi-layer graphene electrodes, Org. Electron. 11 (11) (2010) 1864.

[12] H. Park, J.A. Rowehl, K.K. Kim, V. Bulovic, J. Kong, Doped graphene electrodes for organic solar cells, Nanotechnology 21 (2010) 505204.

[13] L. Valentini, M. Cardinali, S.B. Bon, D. Bagnis, R. Verdejo, M.A. Lopez-Manchado, J.M. Kenny, Use of butylamine modified graphene sheets in polymer solar cells, J. Mater. Chem. 20 (2010) 995.

[14] Y.C. Shih, Y.B. Lan, C.S. Li, H.C. Hsieh, L. Wang, C.I. Wu, K.F. Lin, Amino-acid-induced preferential orientation of perovskite crystals for enhancing interfacial charge transfer and photovoltaic performance, Small 13 (2017) 1604305.

[15] Y.C. Shih, L.Y. Wang, H.C. Hsieh, K.F. Lin, Enhancing the photocurrent of perovskite solar cells via modification of the TiO2/CH3NH3PbI3 heterojunction interface with amino acid, J. Mater. Chem. A 3 (2015) 9133–9136.

[16] F. Ersan, O. Üzengi Aktürk, E. Aktürk, S. Ciraci, Metal-insulator transition and heterostructure formation by glycines self-assembled on defect-patterned graphene, J. Phys. Chem. C 122 (2018) 14598–14605.

[17] J. Bai, X. Zhong, S. Jiang, Y. Huang, X. Duan, Graphene nanomesh, Nat. Nanotech. 5 (2010) 190–194.

[18] A.W. Robertson, C.S. Allen, Y.A. Wu, K. He, J. Olivier, J. Neethling, A.I. Kirkland, J.H. Warner, Spatial control of defect creation in graphene at the nanoscale, nature communications, Nat. Commun. 3 (2012) 1144.

[19] J. Lahiri, Y. Lin, P. Bozkurt, Oleynik II., M. Batzill, An extended defect in graphene as a metallic wire, Nat. Nanotechnol. 5 (5) (2010) 326.

[20] G. Kresse, D. Joubert, From ultrasoft pseudopotentials to the projector augmented-wave method, Phys. Rev. B 59 (1999) 1758–1775.

[21] J.P. Perdew, K. Burke, M. Ernzerhof, Generalized gradient approximation made simple, Phys. Rev. Lett. 77 (1996) 3865–3868.

[22] S. Grimme, Semiempirical GGA-type density functional constructed with a long-range dispersion correction, J. Comput. Chem. 27 (2006) 1787–1799.

[23] H.J. Monkhorst, J.D. Pack, Special points for Brillouin-zone integrations, Phys. Rev. B 13 (1976) 5188–5192.

[24] H.B. Schlegel, Optimization of equilibrium geometries and transition structures, J. Comput. Chem. 3 (1982) 214–218.

[25] G. Kresse, J. Furthmüller, Efficient iterative schemes for ab initio total-energy calculations using a plane-wave basis set, Phys. Rev. B 54 (1996) 11169–11186.

[26] G. Kresse, J. Furthmüller, Efficiency of ab-initio total energy calculations for metals and semiconductors using a plane-wave basis set, Comput. Mater. Sci. 6 (1996) 15–50.

[27] G. Henkelman, B.P. Uberuaga, H.A. Jonsson, Climbing image nudged elastic band method for finding saddle points and minimum energy paths, J. Chem. Phys. 113 (2000) 9901.

[28] The AM1.5G spectrum was taken from the NREL website. http://rredc.nrel.gov/solar/spectra/am1.5.

[29] V. Barone, C. Adamo, F. Lelj, J. Chem. Phys. 102 (1995) 364.

[30] J.H. Jensen, M.S. Gordon, Conformational behavior of gaseous glycine by a density functional approach, J. Am. Chem. Soc. 117 (1995) 8159–8170.

[31] J. Heyd, G.E. Scuseria, M. Ernzerhof, Hybrid functionals based on a screened coulomb potential, J. Chem. Phys. 118 (2003) 8207–8215.

[32] C. Rajesh, C. Majumder, H. Mizuseki, Y. Kawazoe, A theoretical study on the interaction of aromatic amino acids with graphene and single walled carbon nanotube, J. Chem. Phys. 130 (2009) 124911.

[33] C. Cazorla, Ab initio study of the binding of collagen amino acids to graphene and A-doped (A = H, Ca) graphene, Thin Solid Films 518 (2010) 6951–6961.

[34] F. Ma, Z. Zhang, H. Jia, X. Liu, Y. Hao, B. Xu, Adsorption of cysteine molecule on intrinsic and Pt-dopedgraphene: a first-principle study, J. Mol. Struct.: Theochem 955 (2010) 134–139.

[35] H.H. Gürel, V.O. Özçelik, S. Ciraci, Dissociative adsorption of molecules on graphene and silicene, J. Phys. Chem. C 118 (2014) 27574–27582.

[36] H.T. Larijani, M. Jahanshahi, M.D. Ganji, M.H. Kiani, Computational studies on the interactions of glycine amino acid with graphene, h-BN and h-SiC monolayers, Phys. Chem. Chem. Phys. 19 (2017) 1896–1908.

[37] F. Naderi, A. Karami, B. Naderi, The interaction between Glycine and carbon nanostructure, Org. Chem. J. 2 (2010) 44–49.

[38] P.A. Denis, F. Iribarne, Comparative study of defect reactivity in graphene, J. Phy. Chem. C 117 (2013) 19048–19055.

[39] A.W. Robertson, B. Montanari, K. He, C.S. Allen, Y.A. Wu, N.M. Harrison, A.I. Kirkland, J.H. Warner, Structural reconstruction of the graphene monovacancy, ACS Nano 7 (2013) 4495–4502.

[40] K. Momma, F. Izumi VESTA, A three-dimensional visualization system for electronic and structural analysis, J. Appl. Crystallogr. 41 (2008) 653–658.

[41] J. Wang, Y. Xu, H. Chen, B. Zhang, Ultraviolet dielectric hyperlens with layered graphene and boron nitride, J. Mater. Chem. 22 (2012) 15863–15868.

[42] M. Mantina, A.C. Chamberlin, R. Valero, C.J. Cramer, D.G. Truhlar, Consistent van der Waals radii for the whole main group, J. Phys. Chem. A 113 (2009) 5806–5812.

[43] L.G. Bulusheva, O.V. Sadelnikova, A.V. Okotrub, Many-body effects in optical response of graphene-based structures, Int. J. Quant. Chem. 116 (2016) 270–281.

[44] V.G. Kravets, A.N. Grogorenko, R.R. Nair, P. Blake, S. Anissimova, K.S. Novoselov, A.K. Geim, Spectroscopic ellipsometry of graphene and an exciton-shifted van Hove peak in absorption, Phys. Rev. B 81 (2010) 115413.

[45] A. Splendiani, L. Sun, Y. Zhang, T. Li, J. Kim, C.Y. Chim, G. Galli, F. Wang, Emerging photoluminescence in monolayer MoS^2, Nano Lett. 10 (4) (2010) 1271–1275.

[46] M. Bernardi, C. Ataca, M. Palummo, J.C. Grossman, Optical and electronic properties of two-dimensional layered materials, Nanophotonics 5 (2016) 111–125.

[47] D. Saladukha, M.B. Clavel, F.M. Armando, G.G. Diniz, M. Grüning, M.K. Hudait, T.J. Ochalski, Direct and indirect band gaps in Ge under biaxial tensile strain investigated by photoluminescence and photoreflectance studies, Phys. Rev. B 97 (2018) 195304.